[Plant Signaling & Behavior 2:2, 86-95; March/April 2007]; ©2007 Landes Bioscience

Research Paper

Cryptogein-Induced Anion Effluxes

Electrophysiological Properties and Analysis of the Mechanisms Through Which They Contribute to the Elicitor-Triggered Cell Death

Adrien Gauthier[1]
Olivier Lamotte[2]
David Reboutier[3]
François Bouteau[3]
Alain Pugin[1]
David Wendehenne[1,*]

[1]Université de Bourgogne; Plante-Microbe-Environnement; Dijon, France

[2]Department of Plant Biology; Fribourg, Switzerland

[3]Laboratoire d'Electrophysiologie des Membranes; Université Paris; Paris, France

*Correspondence to: David Wendehenne; Université de Bourgogne; Plante-Microbe-Environnement; INRA, 17 rue Sully, BP 86510, 21065; Dijon cedex, France; Tel.: +33.03.80.69.37.22; Fax: +33.03.80.69.32.26; Email: wendehen@dijon.inra.fr

Original manuscript submitted: 11/27/07
Manuscript accepted: 02/15/07

Previously published online as a *Plant Signaling & Behavior* E-publication: http://www.landesbioscience.com/journals/psb/abstract.php?id=4015

KEY WORDS

anion channels, calcium, cell death, cryptogein, plasma membrane depolarization, proteases

ACKNOWLEDGEMENTS

We are grateful to Laurent Barnavon and Annie Buchwalter for helpful discussions and to André Bouchot from the Center of Microscopy (IFR 100, University of Burgundy, Dijon, France). This work was supported by the Ministère de l'Education Nationale, de la Recherche et de la Technologie, and the Conseil Régional de Bourgogne.

ABSTRACT

Anion effluxes are amongst the earliest reactions of plant cells to elicitors of defence responses. However, their properties and their role in disease resistance remain almost unknown. We previously demonstrated that cryptogein, an elicitor of tobacco defence responses, induces a nitrate (NO_3^-) efflux. This efflux is an early prerequisite to the cryptogein-triggered hypersensitive response (HR). Here, we analyzed the electrophysiological properties of the elicitor-mediated NO_3^- efflux and clarified the mechanisms through which it contributes to cell death. Application of the discontinuous single electrode voltage-clamp technique in tobacco cells elicited with cryptogein enabled us to record the activation of slow-type deactivating anion channel currents. Cryptogein-induced plasma membrane depolarization and Ca^{2+} influx, an essential component of elicitor signalling for HR cell death, were prevented by inhibiting the NO_3^- efflux. Similarly, pharmacological blocking of the anion efflux suppressed vacuolar collapse, a hallmark of cell death. The role of NO_3^- efflux in mediating proteases activation was further assessed. It is shown that cryptogein induced the activation of three proteases with apparent molecular masses of 95, 190 and 240 kDa. Their activation occurred independently on the anion efflux and, together with cell death, was strongly reduced by cycloheximide and the protease inhibitor PMSF. In contrast, the NO_3^- efflux was shown to promote the accumulation of transcripts encoding vacuolar processing enzymes, a family of proteases previously reported to contribute to the disruption of vacuole integrity observed during the HR. Collectively, our data indicate that anion efflux is an early prerequisite to morphological and biochemical events participating to cell death.

INTRODUCTION

Plants are constantly challenged with potential pathogenic microorganisms and have evolved a diversity of constitutive and inducible responses in order to resist their aggressors. The inducible responses involve the production of reactive oxygen species (ROS), the strengthening of the cell wall and the transcriptional activation of defence-related genes that encode antimicrobial secondary metabolite-biosynthetic enzymes as well as pathogenesis-related proteins showing antimicrobial properties.[1] Defence genes also encode proteins functioning in the synthesis of salicylic acid (SA), jasmonic acid and ethylene which play a crucial role in the development of systemic resistance to the distal uninfected parts of the plant.[2] In many cases, plant resistance is associated with a rapid, localized cell death at the site of infection called the hypersensitive response.[3] The HR is thought to directly kill the pathogens and/or to limit their spreading by depriving them of access to further nutrient sources. Cell death during the HR has been shown to be genetically programmed and displays apoptosis-like features such as cell shrinkage, chromatin condensation and DNA cleavage.[4] Understanding the mechanisms underlying the HR has been the focus of important research and components of the signalling pathway leading to the HR, together with key cell death executors have recently been identified. Cell death signals include ROS, nitric oxide (NO), SA and proteins related to Ca^{2+} and lipid signaling.[5-8] Cell death executors include proteases such as the vacuolar processing enzymes (VPE), a family of vacuole-localized enzymes showing caspase-1 activity.[8] VPEs are responsible for the proteolytic processing of other vacuolar proteins and might contribute to the disruption of the vacuolar integrity observed during the HR.[9]

Plant defence responses are initiated by the recognition of pathogen-derived molecules called race-specific or general elicitors (also named Pathogen-Associated Molecular Patterns or PAMPs), depending on the patho-system.[10] Cryptogein, a 10 kDa

proteinaceous elicitor secreted by the oomycete *Phytophthora cryptogea*, has been extensively used to investigate the molecular mechanisms underlying disease resistance in tobacco. Cryptogein belongs to the family of elicitins, which are small proteins secreted by *Phytophthora* and *Pythium* species.[11] Upon application to tobacco leaves, cryptogein triggers the expression of defence-related genes, an HR-like response and a systemic resistance against various pathogens including *Phytophthora parasitica* var. *nicotianae*, the causal agent of the black shank disease.[12] Cryptogein binds to plasma membrane high affinity binding sites showing biochemical properties expected from a receptor.[13-14] Using tobacco cell suspensions and a combination of biochemical, pharmacological and molecular methods, components involved in the transduction pathway coupling cryptogein recognition to the activation of defence responses have been identified, namely changes in plasma membrane permeability, activation of an NADPH oxidase responsible for ROS production and cytosol acidification, activation of protein kinases including MAPKs, disruption of the microtubular cytoskeleton and NO synthesis.[15] The interaction between these early signalling components appears to be complex and there is evidence that their activation directly correlates with a transient increase in cytosolic free Ca^{2+} concentration ($[Ca^{2+}]_{cyt}$).[6,16] Recent studies also highlight the occurrence of a positive feedback between NO and Ca^{2+} and their respective involvement in the elicitor-triggered defence gene expression and cell death.[6,17-18] In contrast, several lines of evidence indicate that ROS do not contribute to cryptogein-triggered cell death.[19-20]

Plant anion channels play fundamental roles in key biological processes including turgor regulation, nutrient acquisition, membrane potential regulation and signal transduction.[21] Several types of anion channels differing in their voltage dependence, kinetic properties and anion selectivity have been characterized, mostly by electrophysiological techniques.[22] Depending on the type of anion channels, their regulation involved free cytosolic Ca^{2+}, intracellular nucleotides and phosphorylation events.[22] Anion effluxes, mainly chloride (Cl^-), are amongst the earliest responses observed in plant cells following recognition of pathogenic signals.[1] Despite this, little attention has been paid to their characterization and the consequences of their activation in plant defence responses. We previously reported that cryptogein induced a rapid and massive nitrate (NO_3^-) efflux regulated by Ca^{2+} and phosphorylation-dependent events.[23] The cryptogein-induced NO_3^- efflux was sensitive to structurally unrelated anion channel inhibitors including niflumic acid, glibenclamide, ethacrynic acid, anthracene-9-carboxylic (9-AC) acid and diphenylamine-2-carboxylic acid; niflumic acid and glibenclamide being the most efficient. This efflux led to a loss of intracellular NO_3^- content of about 60% and the concomitant increase of extracellular NO_3^- concentration did not result from a balance between NO_3^- efflux and NO_3^-/H^+ symporter-mediated NO_3^- influx. Interestingly, the NO_3^- efflux was shown to be necessary for the mediation of cryptogein-induced defence responses including the oxidative burst, the induction of defence-related genes and the development of the HR. The involvement of the NO_3^- efflux as a critical component of the cell death process reminds the key role of anion channels in apoptosis in animals. Indeed, several studies have reported that in various types of mammalian cells, plasma membrane Cl^- channel activation is an early prerequisite to apoptotic events including cell shrinkage (termed AVD for apoptotic volume decrease), cytochrome c release, proteases (including caspases) and nucleases activation and, ultimately, cell death.[24-25]

Taken together, these data suggest that anion efflux is not a passive secondary feature of plant defence responses, but a driver of this process. However, the corresponding ion channel activities have rarely been recorded. As a matter of fact, most of the electrophysiological studies on plant cells are performed using the patch-clamp technique applied to protoplasts, but removing the cell wall during protoplast preparation is likely to alter the capacity of the cells to respond to pathogens or elicitors (our personal observation and refs. 26 and 27). Another approach to analyze ion channels in intact cells is the microelectrode voltage-clamp technique. This technique allows recording of the free running membrane potential and whole cell ion currents without disturbing cell functioning and the intracellular medium.

In the present study we undertook an electrophysiological analysis of the cryptogein-induced anion effluxes using the single microelectrode voltage-clamp technique (SEVC) and analysed the downstream dependent events leading to cell death. Our data indicate that the elicitor-mediated anion current could allow important anion effluxes as described for guard cell slow (S)-type anion channels. Furthermore, the NO_3^- efflux is part of the mechanisms leading to plasma membrane depolarization, Ca^{2+} influx, vacuole shrinkage and *VPEs* transcripts accumulation.

MATERIALS AND METHODS

Cell culture. *Nicotiana tabacum* cv Xanthi cells were cultivated as previously described.[18] Briefly, cell suspensions were maintained in Chandler's medium (Chandler[28]) under continuous light (photon flux rate 30–40 μmol m^{-2} s^{-1}) on a rotary shaker (150 rpm) and at 25°C. Cells were maintained in the exponential phase and used for elicitor treatment 1 day after subculturing.

Nicotiana plumbaginifolia cell suspensions expressing apoaequorin[6] were maintained in Chandler's medium and cultivated in the dark on a rotary shaker (150 rpm) at 25°C. Cell suspensions were used for the analysis of cytosolic free calcium concentrations 8 days after subculturing.

Cell culture treatment. All the pharmacological compounds were purchased from Sigma-Aldrich (Saint-Quentin-Fallavier, France) except coelenterazine from Calbiochem (Schwalback, Germany). Antipain, leupeptin, cycloheximide, Z-Val-Ala-Asp(OMe) fluoromethylketone (Z-FAD-fmk) and coelenterazine were dissolved in water. Glibenclamide, benzylsulfonyl fluoride (PMSF) and Bis(1,3-dibarbituric acid)-trimethine ($DiBAC_4$) were prepared in dimethyl sulfoxide (DMSO). Niflumic acid was dissolved in 4% DMSO solution alkalinized by KOH. Appropriate controls were performed to ensure that DMSO did not interfere with the experiment. Cryptogein was purified according to Bonnet et al[29] and prepared as a 10 μM stock solution in water.

Treatment of cell suspensions was carried out as described previously.[18] Briefly, cells were washed twice and resuspended at 0.1 g fresh weight/mL in the H10 suspension buffer (175 mM mannitol, 0.5 mM $CaCl_2$, 0.5 mM K_2SO_4 and 10 mM Hepes, pH 5.75) and equilibrated for 1 h at 24°C on a rotary shaker (150 rpm). For northern blot experiments, cell suspensions were kept in Chandler's medium during cryptogein treatment. The pharmacological compounds were added 10 min before the elicitor.

Extracellular nitrate content analysis. At the indicated time of cryptogein treatment, aliquots of 2 mL of cells (0.2 g fresh weight) were filtrated and the resulting extracellular medium was collected. The NO_3^- concentration in the extracellular medium was determined using a NO_3^- colorimetric assay kit (Alexis Biochemicals).[23]

Single electrode voltage clamp assays. Tobacco cells were impaled in H50 medium (175 mM mannitol, 0.5 mM $CaCl_2$, 0.5 mM K_2SO_4 and 50 mM Hepes, pH 5.75) with borosilicate capillary glass (Clark GC 150F) micropipettes (resistance: 50 MΩ when filled with 600 mM KCl). Individual cells were voltage-clamped using an Axoclamp 2B amplifier (Axon Instruments, Foster City, CA, USA) for discontinuous single electrode voltage clamp experiments (Finkel & Redmann, 1984) as previously described for *A. thaliana* cells.[30] Voltage and current were digitized with a computer fitted with a Digidata 1320A acquisition board (Axon Instruments). The electrometer was driven by pClamp software (pCLAMP8, Axon Instruments). The experiments were conducted at 22 ± 2°C on 4-day-old cells.

When recording were performed in H10 medium in the absence of cryptogein, two tobacco cell populations could be discriminate (data not shown). One with hyperpolarized membrane potentials around -110 mV, thus near from the equilibrium potential estimated for K^+. These cells displayed predominant outward rectifying time dependent K^+ current which nature was confirmed by tail current analysis (data not shown). The second cell population had a plasma membrane potential around -50 mV, thus far from EK^+, and the main current recorded on these cells present the hallmarks of anion channel currents. The second population of cells was dominant in H50 medium. Therefore, all the recordings were performed using H50 medium. Such different populations of cells were already reported on *Arabidopsis thaliana*.[30]

Measurement of plasma membrane depolarization by fluorescence. Plasma membrane depolarization was monitored using the fluorescent probe $DiBAC_4$ according to Lamotte et al.[17] with slight modifications. After equilibration for 1 h at 24°C in the suspension buffer, cells were incubated with $DiBAC_4$ for 30 min in the dark. Then, 1.5 mL of cells was transferred to a cuvette and treated with cryptogein. During the measurements, cells were maintained under low shaking to avoid sedimentation. $DiBAC_4$ fluorescence was recorded continuously at 4-s intervals using a fluorometer (SAFAS flx-Xenius, SAFS-Monaco) with 490 nm excitation and 510 nm emission filters. Fluorescence was expressed as relative fluorescence units. The assays did not exceed 30 min.

$DiBAC_4$ fluorescence was visualized using a Zeiss Axio Vert 200M inverted fluorescence microscope. Digital images were captured with a cool charged-coupled device camera controlled with AxioVision software (Zeiss).

Ca^{2+} influx measurement. Ca^{2+} influx measurements were performed as reported by Tavernier et al[16]. $^{45}Ca^{2+}$ (0.033 MBq g^{-1} of fresh weight of cells) was added to cell suspensions 15 min before cryptogein treatment. At the indicated time, duplicate samples of 2 mL were taken from the batch of treated cell suspensions, filtered under vacuum, and washed on GF/A glass-microfiber filters (Whatman, Clifton, NJ) once for 1 min and twice for 20 s with 10 mL of washing buffer (175 mM mannitol, 0.5 mM K_2SO_4, 2 mL $LaCl_3$ and 10 mM Hepes, pH 5.75). Then, the cells were transferred to scintillation vials and weighted before adding 10 mL of ready Safe Cocktail (Beckman Instruments, Fullerton, CA). Finally, the vials were shaken and counted in a scintillation counter (TRI-CARB 2100 TR, Packard Instrument, Rungis, France).

Determination of cytosolic free calcium concentrations. Analysis of cytosolic free calcium concentrations were performed using *Nicotiana plumbaginifolia* cell suspensions expressing apoaequorin.[6] In vivo reconstitution of aequorin was performed by addition of 1 μM coelenterazine to cells maintained in H10 medium for at least 3 h in the dark (150 rpm, 24°C). Coelenterazine is a prosthetic group of aequorin required for its full Ca^{2+}-binding activity. The bioluminescence of 250-μL aliquots of cells (maintained in a cuvette) was recorded continuously at 1-s intervals using a digital luminometer (Lumat LB9507, Berthold, Bad Wildbad, Germany). At the end of the experiments, residual functional aequorin was quantified by adding 300 μL of lysis buffer (10mM $CaCl_2$, 2% Nonidet-P40, v/v, 10% ethanol, v/v) and monitoring the resulting increase in luminescence. Luminescence data transformation into cytosolic Ca^{2+} concentration was calculated as previously described.[6]

Measurement of vacuole volume loss and cell death. At the indicated time, duplicate samples of 1 mL were taken from the batch of treated cell suspensions, washed two times with 1 mL of H10 equilibrated at pH 7.0, and then incubated for 5 min in the same solution containing 0.01% of neutral red, a vital dye that accumulates in the acidic vacuole. Then, cells were observed using a Leica DMRB microscope (Leica, Wetzlar, Germany). Cells showing a loss of vacuole volume were counted and expressed as a % of total cells. Cells that did not accumulate neutral red were considered dead. One thousand cells were counted for each treatment.

In-gel protease assay. In-gel protease assays were performed according to Solomon et al.[31] with modifications. Briefly, at the indicated time, 2.5 mL of cell suspensions (0.25 g) were harvested from the batch of treated cell suspensions, filtered under vacuum and frozen in liquid nitrogen. Cells were ground in a mortar and resuspended in 450 μL of extraction buffer (250 mM sucrose, 2 mM DTT, 50 mM Tris-HCl, pH 7.8). Cell walls and insoluble matter were removed by centrifugation (4°C, 15,000 *g*, 20 min). Then, 350 μL of the supernatant were added to 70 μL of Laemmli loading buffer (0.5% bromophenol blue, 50% glycerol, 0.075% DTT, 0.1% SDS, 315 mM Tris HCl, pH 6.8). The concentration of proteins was determined according to Bradford.[32] The samples (60 μg of proteins) were incubated at 42°C for 20 min before loading on an SDS-polyacrylamide gel (4–8% gradient) containing 0.2% of gelatin as the protease substrate. After migration, proteins were renatured by two washes (45 min each) of the gel in a 50 mM Tris HCl, pH 7.8 buffer containing 2% of Triton X-100. Then, the gel was incubated 16 h at 37°C in the activity buffer (5 mM $CaCl_2$, 5 mM DTT, 50 mM Tris-HCl, pH 7.8) and stained with Coomassie Brillant Blue R 250. Active proteases digested the gelatin and appeared as white bands. After staining, the gels were scanned (Amersham Biosciences Image Scanner, software LabScanTM 5.0), converted to a grayscale mode, and inverted with Adobe PhotoShop (Adobe Systems Inc., San Jose, CA).

Cloning of the *NtVPE-1b* 712 bp cDNA fragment and northern blot experiments. cDNA from tobacco cells treated with cryptogein (50 nM) for 4 h was prepared and used as a template to isolate a 712 bp cDNA fragment corresponding to *NtVPE-1b*. The oligonucleotide primers used were (5'-3') GGGTGGTCTGAAAGATGAG (forward) and (5'-3') GTATAGAGCATCCTTGCTG (reverse). These primers were designed according to Hatsugai et al (2004). The 712 bp PCR fragment was cloned into a pCRII-TOPO vector and sequenced (Sequencing Service of Dijon Campus: CERCOBIO). The identity of the 712 bp PCR fragment was confirmed through BLAST analysis.

For RNA gel blot analysis, total RNA was extracted from cell cultures using Trizol reagent (Gibco BRL) according to the supplier's instructions. Ten μg of total RNA per lane were separated on 1.2% agarose gels (w/v) containing 1.1% formaldehyde (w/v), blotted to a nylon membrane (Hybond-XL Amersham Biosciences, Piscataway,

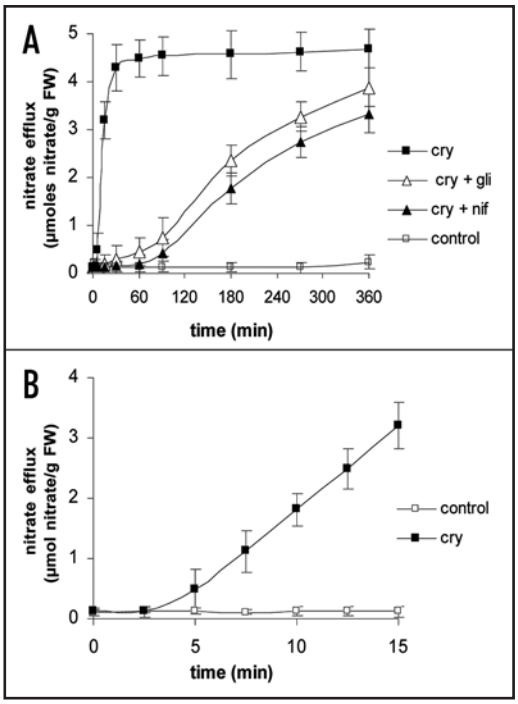

Figure 1. Cryptogein induced NO_3^- efflux. (A) Time course of NO_3^- efflux induced by cryptogein. Niflumic acid (200 µM) and glibenclamide (200 µM) were added to cell suspensions 10 min before cryptogein (25 nM). After cryptogein addition, external medium aliquots were taken at the times indicated. Nitrate content was determined using a colorimetric assay. Glibenclamide alone and niflumic acid alone, omitted for clarity, did not induce any NO_3^- efflux during the time of experiment. (B) Detail of the early time course of cryptogein induced NO_3^- efflux. Each value represents the mean ± SD of 15 measurements (three replicates per experiment performed five times). cry, cryptogein; gli, glibenclamide; nif, niflumic acid; FW, fresh weight.

NJ, USA), and cross-linked by UV light. The 712 bp cDNA fragment corresponding to *NtVPE-1b* used as a probe for hybridization was labelled by random priming (Ready-To-Go DNA Labelling Beads-dCTP, Amersham Biosciences,). Membrane hybridization was performed at 65°C as described by Church and Gilbert.[33] The membrane was washed with 2X SSC (1X SSC is 0.15 M NaCl and 0.015 M sodium citrate; pH 7) twice for 5 min at room temperature, with 0.5% SDS (w/v) and 2X SSC twice for 30 min at 65°C, and subsequently with 0.1 X SSC twice for 30 min at room temperature. The membrane was exposed to X-Omat AR film (Kodak).

RESULTS

Effect of cryptogein on anion efflux in tobacco cells. As previously reported,[23] cryptogein induces a large NO_3^- efflux in tobacco cell suspensions that occurs within 5 min (Fig. 1A and B). After 60 min, the NO_3^- efflux reaches a maximum corresponding to 4.5 ± 0.4 µmol/g fresh cells. The anion efflux is transiently inhibited by niflumic acid and glibenclamide, two structurally unrelated anion channel blockers.

The electrophysiological properties of the cryptogein-induced anion efflux were investigated using the SEVC technique. Under control conditions in H50 medium, successful impalements were routinely obtained in turgid tobacco cultured cells. In response to cryptogein, the main current recorded displayed a slow deactivation upon hyperpolarization and a current voltage relationship (Fig. 2A

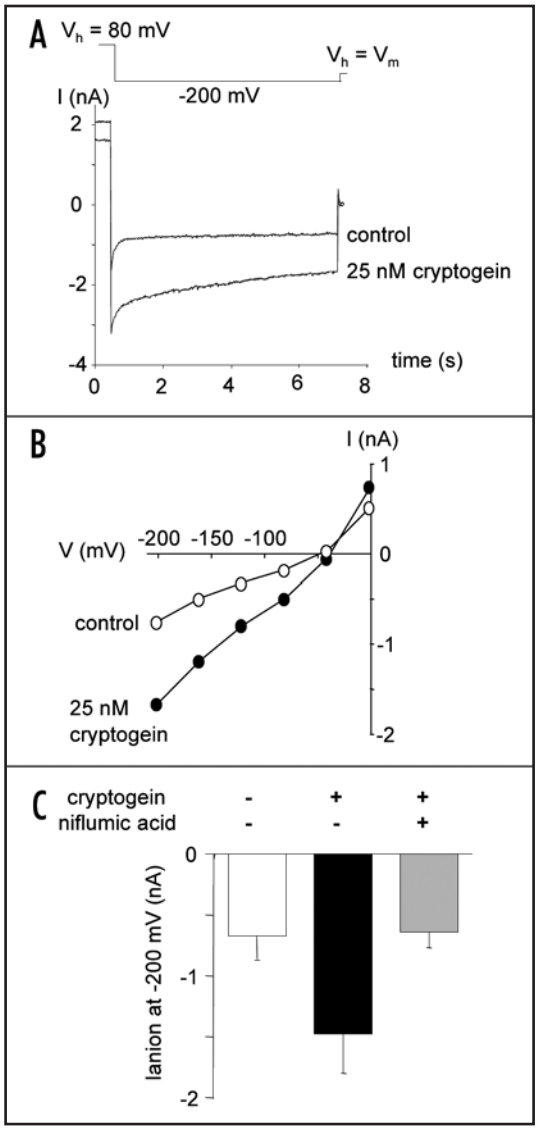

Figure 2. Cryptogein induced changes in anion currents in tobacco cells. (A) Recording of anion current elicited at -200 mV after a depolarizing voltage step of +80 mV. The deactivating currents were measured before and after addition of 25 nM cryptogein (V_h, holding potential; V_m, membrane potential). (B) Current-voltage relationships. The steady-state current amplitudes were measured at membrane potentials ranging from -200 to 0 mV before and after addition of 25 nM cryptogein. For figure (A and B), results are from one of nine representative experiments. (C) Anion current (at steady state and -200 mV) in control condition (white bar), after addition of 25 nM cryptogein (black bar) and after a subsequent addition of 200 µM niflumic acid (grey bar). Mean values ± SD were recorded from at least four cells.

and B) resembling the one described for guard cell slow-type anion channels[34] and anion currents of *A. thaliana* suspension cells,[30] although some of the instantaneous currents could be carried by fast-activating anion currents as described in guard cells.[35] The increase in anion currents occurred after a lag phase of 4.1 ± 1.3 min following the application cryptogein (n = 9, data not shown). These currents were sensitive to niflumic acid (Fig. 2C) and also to glibenclamide and two other anion channel blockers previously reported to transiently inhibit the cryptogein-induced NO_3^- efflux,[23] namely 9-AC and NPPB (data not shown). Therefore, anion channels are good candidates for the mediation of these slow deactivating currents.

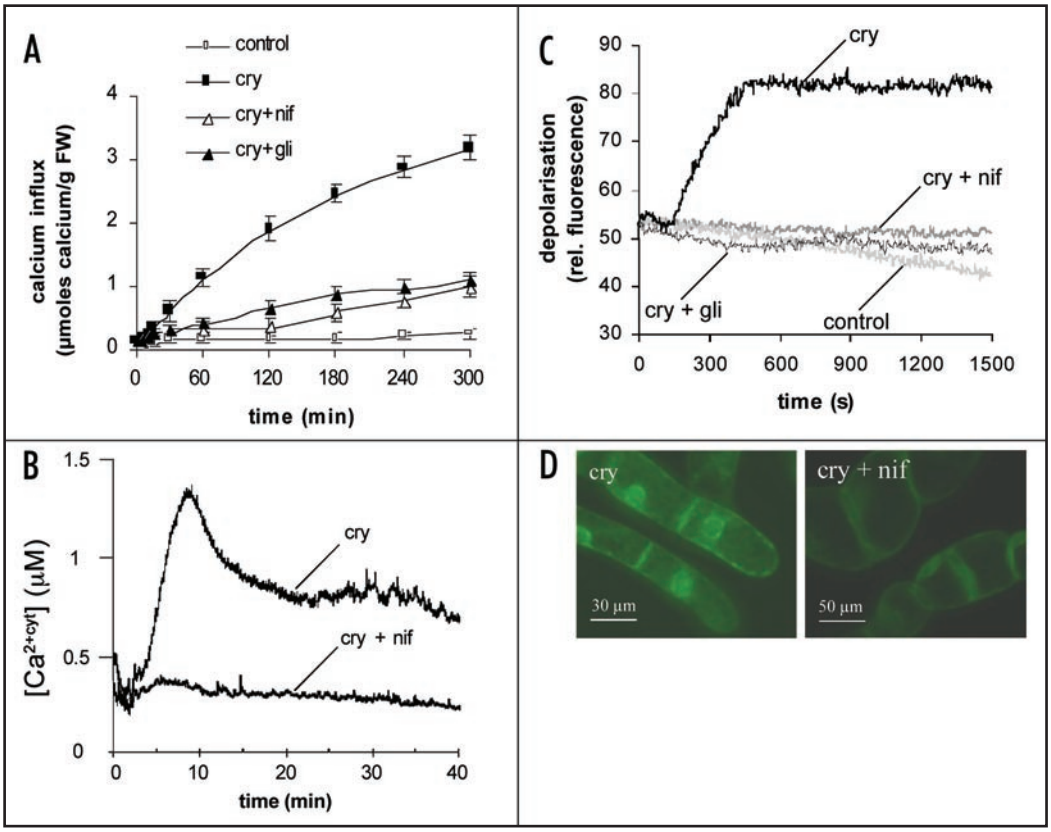

Figure 3. Cryptogein-induced NO_3^- efflux contributes to plasma membrane depolarisation and Ca^{2+} influx. (A) Effect of niflumic acid and glibenclamide on cryptogein-mediated extracellular Ca^{2+} influx. Cells were preincubated with $^{45}Ca^{2+}$ 5 min before the addition of 200 µM niflumic acid or 200 µM glibenclamide. Cryptogein was added 10 min after the anion channel inhibitors. Aliquots of cells were taken from treated cell suspensions at the times indicated and withdrawn. Ca^{2+} influx was determined as described in experimental procedures. Glibenclamide alone and niflumic acid alone, omitted for clarity, did not induce any Ca^{2+} influx during the time of experiment. Each value represents the mean ± SD of nine measurements (three replicates per experiment performed three times). (B) Effect of niflumic acid on cryptogein-induced $[Ca^{2+}]_{cyt}$ increase in apoaequorin-transformed *N. plumbaginifolia* cells. Niflumic acid (200 µM) was added to cell suspensions 10 min prior to cryptogein (1 µM). $[Ca^{2+}]_{cyt}$ was measured as detailed under Material and methods. Niflumic acid alone, omitted for clarity, did not induce changes in $[Ca^{2+}]_{cyt}$ during the time of experiment. Results are from one of four representative experiments. (C) Time course of plasma membrane potential changes in tobacco cells treated with cryptogein. Niflumic acid (200 µM) and glibenclamide (200 µM) were added to cell suspensions 10 min before cryptogein (25 nM). Changes in membrane potential were measured by following $DiBAC_4$ fluorescence. Glibenclamide alone and niflumic acid alone, omitted for clarity, did not induce any changes of $DiBAC_4$ fluorescence during the time of experiment. These data are representative of five experiments. (D) Fluorescence of $DiBAC_4$ in response to cryptogein. Tobacco cells were loaded with $DiBAC_4$ and treated with cryptogein (25 nM). Niflumic acid (200 µM) was added to $DiBAC_4$-loaded cell suspensions 10 min prior to cryptogein. Results are from one of three representative experiments. Cry, cryptogen; gli, glibenclamide; nif, nifflumic acid; FW, fresh weight.

The cryptogein-induced anion efflux determines plasma membrane depolarization and contributes to Ca^{2+} influx. It has previously been reported that the cryptogein-induced Ca^{2+} influx is an essential component of elicitor signalling for HR cell death.[6-19] Kadota et al[36] also provided genetic evidence that the Ca^{2+} influx contributing to the elicitor-induced cell death might be mediated by voltage-dependent Ca^{2+} permeable channels homologous to mammalian two-pore channels. To explore the hypothesis that the NO_3^- efflux might participate in cell death by promoting the mobilization of Ca^{2+}, niflumic acid and glibenclamide were tested for their effects on the elicitor-induced Ca^{2+} influx and plasma membrane depolarization. The Ca^{2+} influx was investigated using $^{45}Ca^{2+}$ as a tracer (Fig. 3A). In accordance with our previous studies[6,16,18] cryptogein induced a rapid extracellular Ca^{2+} uptake which increased continuously during the 5 h of experiments. The Ca^{2+} influx was strongly affected by niflumic acid and glibenclamide, indicating that the anion efflux seems essential for the Ca^{2+} influx.

We next investigated the effect of niflumic acid on cryptogein-mediated changes in $[Ca^{2+}]_{cyt}$ using transgenic *N. plumbaginifolia* cell suspensions expressing the Ca^{2+} reporter apoaequorin in the cytosol. We previously reported that when used at 1 µM, cryptogein triggers the same signaling cascade in *N. plumbaginifolia* and in *N. tabacum* cell suspensions.[6] As reported by Lecourieux et al,[6] cryptogein induced a specific cytosolic Ca^{2+} signature characterized by an first and transient increase of $[Ca^{2+}]_{cyt}$ reaching 1.3 µM after 8 min, followed by a second and more prolonged sustained $[Ca^{2+}]_{cyt}$ increase which peaked at 0.8 µM after 30 min (Fig. 3B) and lasted at least 2 h (data not shown). Niflumic acid, added 10 min before cryptogein treatment, clearly suppressed the elicitor-induced increase in $[Ca^{2+}]_{cyt}$. Similarly, glibenclamide inhibited almost completely cryptogein-triggered $[Ca^{2+}]_{cyt}$ increase (data not shown). These results indicate that the NO_3^- efflux is a component of the signaling cascade leading to cryptogein-induced changes of $[Ca^{2+}]_{cyt}$.

Depolarization was investigated using the voltage-sensitive dye $DiBAC_4$, an anionic fluorophore which has been successfully used to monitor changes in plasma membrane potential accompanying plant cell responses to elicitors and nitric oxide.[17,37] $DiBAC_4$ enters depolarized cells where it interacts with lipid membranes and proteins, resulting in a raise in fluorescence.[38] Following application of cryptogein, an increase in fluorescence occurred after a lag phase of 3 min, indicating plasma membrane depolarization (Fig. 3C). After 7.5 min, the increase in fluorescence reached a maximum and did not decrease for the next 18 min of the experiment. As expected, $DiBAC_4$ fluorescence was distributed along the plasma membrane and in the cytosol (Fig. 3D). Niflumic acid and glibenclamide blocked the increase in fluorescence induced by cryptogein (Fig. 3C and D), suggesting that the anion efflux is involved in plasma membrane depolarization.

The cryptogein-induced anion efflux participates in pathways leading to vacuole shrinkage and *VPE* genes expression. Vacuole shrinkage is a morphological feature of cells undergoing HR-like

Table 1 **Effects of protease inhibitors, anion channel inhibitors and cycloheximide on cryptogein-induced proteases activation and cell death**

Inhibitors	P240	P190	P95	Inhibition of Cell Death (%)
Protease inhibitors				
- antipain[a]	+	+	+	nd
- leupeptin[a]	-	-	+/-	nd
- Z-FAD-fmk	-	-	-	20 ± 8
- PMSF	+	+	+	75 ± 7
Anion channel inhibitors				
- niflumic acid	-	-	-	35 ± 3
- glibenclamide	-	-	-	26 ± 3
cycloheximide	+	+	+	86 ± 9

PMSF (500 μM), antipain (50 μM), leupeptin (25 μM), Z-FAD-fmk (0.1 μM), niflumic acid (200 μM), glibenclamide (200 μM) and cycloheximide (50 μM) were added to the cell suspensions 10 min before cryptogein (25 nM). Cryptogein-induced cell death was estimated after 28 h, proteases activation was estimated 8, 16, 20 and 28 h after the addition of the elicitor to the cell suspensions. When used alone, PMSF and Z-FAD-fmk did not induce cell death; antipain and leupeptin induced 30 to 35% cell death after 28 h. -, no effect; +, total inhibition; +/-, partial and poorly reproducible inhibition; [a], toxic effects (antipain and leupeptin alone induced significant cell death); nd, not determined because of the toxicity of the inhibitor used

cell death.[4] The molecular mechanisms that trigger this process have been poorly investigated. Figure 4A shows that after 1.5 h of cryptogein treatment, about 27% of the cells displayed a loss of vacuolar volume. The percentage of cells showing vacuole shrinkage increased with time and reached 65 ± 8% after 10 h. Then the number of cells exhibiting vacuole volume loss decreased together with the increase of cell death which reached 40% after 28 h of elicitor treatment (Fig. 4B). Figure 4C shows representative morphologies of tobacco cells treated with the elicitor for 28 hr and colored with the vital vacuolar dye neutral red. Compared with control cells, strong vacuole shrinkage is observed in most of the cells and some of them are dead. In the presence of niflumic acid and glibenclamide, the percentage of cells showing vacuole shrinkage after a 90 min cryptogein treatment was reduced by 80% and 73%, respectively (Fig. 4A). With longer treatment, an attenuation of the inhibitory effect was observed, about 47% and 35% of inhibition being obtained after 28 h, respectively. This attenuation might be explained by the transient inhibitory effect of the anion channel inhibitors. As previously reported,[23] niflumic acid and glibenclamide also reduced elicitor-mediated cell death by 35% and 26% after 28 h, respectively (Fig. 4B, Table 1). Taken together, these data suggest that anion efflux is a critical component of the elicitor-induced vacuole shrinkage and cell death.

In mammalian cells undergoing apoptosis, the ion efflux (mainly Cl^- and K^+) associated with AVD now appears as a critical component of the cell death process.[24] In particular, the ion loss triggers protease activity. Based on these studies, and on our finding that anion channel activity is intimately involved in mediating vacuole shrinkage and cryptogein-triggered cell death (Fig. 4), we investigated whether the elicitor-induced anion efflux could be a key event in a signalling cascade leading to protease activation. To address this question, protein extracts from cells treated with cryptogein and/or niflumic acid or glibenclamide were assayed in-gel for proteolytic activity with gelatin as a substrate. As shown in Figure 5A, three proteases with apparent molecular masses of 105, 115 and 130 kDa, respectively, were constitutively active in protein extracts from both control and cryptogein-treated cells. In protein extracts from the elicitor-treated cells, three additional active proteases with apparent molecular masses of 95, 190 and 240 kDa (named P95, P190 and P240, respectively) were detected. The P190 and P240 proteases were active after 8 h, their activity slightly increasing with time. The proteolytic activity of P95 was not detected before 20 h of cryptogein treatment but showed a clear time-dependence, a maximum of activity being observed after 28 h. In several experiments, cryptogein also slightly induced the activation of an additional protease with a molecular mass of 210 kDa (Fig. 5A).

Table 1 summarizes the effects of protease inhibitors, cycloheximide and anion efflux blockers on the cryptogein-induced proteolytic activity of P95, P190 and P240 and cell death. The pre-treatment of cells with antipain, a cysteine/serine protease inhibitor led to a complete inhibition of the proteolytic activity of all proteases. Leupeptin, another cysteine/serine protease inhibitor, reduced the protease activity of P95 but did not affect P240 and P190 activities. However, when used alone, both compounds induced cell death (about 30 to 35% after 28 h, data not shown) and, consequently, no link between their inhibitory effects on the proteases and cell death could be determined. Z-FAD-fmk, a general caspase inhibitor, did not counteract the proteolytic activity of P95, P190 and P240 but lowered cell death by 20%. PMSF, an irreversible inhibitor of serine proteases[39] blocked the proteolytic activity of all proteases together with a strong reduction of cell death. Interestingly, in the presence of cycloheximide, a widely-used inhibitor of protein synthesis, the proteolytic activity of the three proteases was completely suppressed, suggesting that these proteases might be first regulated at the transcriptional levels in response to cryptogein. Furthermore, cycloheximide dramatically reduced cell death by almost 86%, pointing out that this process depends mainly on de novo protein synthesis. Finally, when tobacco cells were cotreated with cryptogein and the NO_3^- efflux inhibitors niflumic acid or glibenclamide, the P95, P190 and P240 remained fully active. Therefore, the activation of all three proteases does not seem regulated by an anion efflux-dependent pathway.

The observation that the caspase inhibitor Z-FAD-fmk partly diminished cryptogein-triggered cell death (Table 1) led us to examine a putative role for the anion efflux in mediating the accumulation of mRNA encoding VPEs. Indeed, VPE was recently identified as a vacuolar cysteine protease of 40 kDa showing caspase-1 activity and sensitive to various caspase inhibitors.[8,40] This protease was shown to be essential for HR induction in tobacco challenged by pathogens (including Tobacco Mosaic Virus, TMV) and might regulate cell dismantling during the HR.[8,9,40] Four VPE genes have been identified in tobacco, namely *NtVPE-1a*, *NtVPE-1b*, *NtVPE-2* and *NtVPE-3*.[8] Both mRNA and protein levels of each VPE were shown to be rapidly and transiently increased in response to TMV.[8] To investigate the involvement of VPEs in cryptogein-induced effects in tobacco, we first cloned a 712 bp cDNA corresponding to *NtVPE-1b* and showing 93, 86 and 84% identity with *NtVPE-1a*, *NtVPE-3* and *NtVPE-2* cDNAs, respectively. We next analyzed *VPEs* mRNA accumulation in cryptogein-treated cells by northern blotting using the 712 bp *NtVPE-1b* cDNA fragment as a probe. Supporting the participation of VPEs in cryptogein-induced effects in tobacco, mRNA level of *VPEs* was rapidly and transiently increased in response to the elicitor: mRNA began to accumulate within

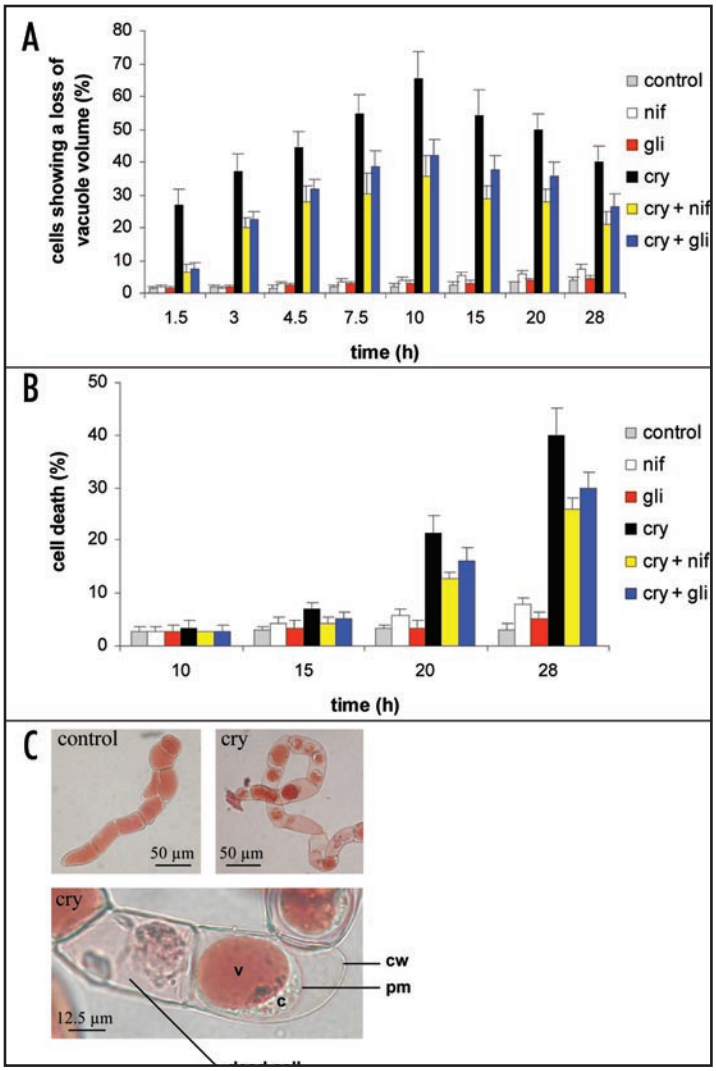

Figure 4. Cryptogein-induced NO_3^- efflux acts upstream of vacuolar collapse. (A) Percentage of cells displaying significant loss of vacuole volume over time in tobacco cells treated with cryptogein. Niflumic acid (200 µM) and glibenclamide (200 µM) were added to cell suspensions min before cryptogein (25 nM). Aliquots of cells were taken from treated cell suspensions at the indicated times and the percent of cells showing significant loss of vacuole volume was estimated by staining with neutral red. Each value represents the mean ± SD of 18 measurements (three replicates per experiment performed six times). (B) Cryptogein-induced cell death is reduced by inhibitors of NO_3^- efflux. Cell suspensions were pretreated for 10 min with niflumic acid (200 µM) or glibenclamide (200 µM) before addition of cryptogein (25 nM). The percentage of dead cells was estimated at the indicated time by staining with neutral red. Each value represents the mean ± SD of 18 measurements (three replicates per experiment performed six times). (C) Light micrograph of cryptogein-treated tobacco cells. Tobacco cells were treated with cryptogein (25 nM) for 28 h and stained with neutral red before observation. Results are from one of six representative experiments. c, cytoplasm; cry, cryptogein; cw, cell wall; gli, glibenclamide; nif, niflumic acid; v, vacuole.

90 min, reached a maximum abundance after 3 h and was barely detectable after 9 h (Fig. 5B). Only one band was detected. When tobacco cells were treated with cryptogein and niflumic acid, *VPEs* transcripts accumulation was reduced, delayed and showed the highest accumulation after 9 h (Fig. 5C). In the presence of glibenclamide, cryptogein-mediated *VPEs* mRNA accumulation was slightly observed after 3 h, showed a maximum of accumulation after 9 h and was still detected after 12 h. Therefore, although the effects of niflumic acid and glibenclamide were slightly different, both compounds delayed the accumulation of *VPEs* transcripts, indicating that this process is dependent, at least partly, on the activation of the NO_3^- efflux.

DISCUSSION

We previously showed that cryptogein activated a fast NO_3^- efflux involved in cell death.[23] In the present study, we investigated the electrophysiological properties of the elicitor-induced NO_3^- efflux and analyzed the mechanisms through which it participate to cell death. We provided evidence that this anion efflux is an early prerequisite to morphological and biochemical events participating to cell death including Ca^{2+} influx, vacuole collapse and *VPE*s transcripts accumulation.

Using the SEVC technique, an increase in anion currents occurred after a lag phase of 4.1 ± 1.3 min following the application of cryptogein to cell suspensions. Upon hyperpolarization conditions, these currents showed a slow-type deactivation resembling the one described for anion currents of *A. thaliana* suspension cells[30] and S-type anion channels supposed to be responsible for long-term anion efflux and depolarization in guard cells.[34] Adding niflumic acid during the cryptogein treatment strongly reduced the anion current. Similarly, pretreatment of the cells with niflumic acid completely prevented the elicitor-induced NO_3^- efflux and the plasma membrane depolarization. Taken together, these data suggest that the slow deactivating anion channel currents might be responsible for the NO_3^- efflux. Supporting this hypothesis, we found that the elicitor-induced increase of anion currents and NO_3^- efflux occurred after a similar lag period of about 4 min (Figs. 1 and 2).

Plasma membrane depolarization constitutes a common early event in the signalling cascade mediating elicitor-induced defence responses in plants. Using the fluorescent probe $DiBAC_4$, we showed that upon cryptogein treatment the plasma membrane potential depolarized according to Pugin et al.[41] The depolarization occurred within 3 min and was concomitant with the detection of the NO_3^- efflux. Supporting a functional link between these two cryptogein-induced early events, we provided evidence that the NO_3^- efflux might be the primary depolarizing factor in cryptogein signalling since niflumic acid and glibenclamide strongly affected the elicitor-induced membrane potential change. Such causal link has been described in blue light signal transduction in *Arabidopsis* hypocotyls in which NPPB, a potent anion channel inhibitor, has been shown to block the stimulus-induced depolarization.[42] Similarly, activation of rapid- and/or S-type anion channels by ABA has been shown to lead to the plasma membrane depolarization of guard cells in *Vicia faba* and *Arabidopsis thaliana*.[43-45] In this model, the long-term anion efflux and sustained depolarization has mainly been attributed to the activity of S-type anion channels. This latter datum, together with the finding that cryptogein induces slow deactivating anion currents and a massive nitrate efflux, suggests that the mechanism by which cryptogein promotes plasma membrane depolarization may resemble those occurring in ABA signalling.

Our results indicate that the activation of the NO_3^- efflux contributes to the vacuole volume loss observed in cryptogein-treated cells. The observation that niflumic acid and also glibenclamide did not completely suppress cryptogein-triggered vacuole shrinkage might be explained by the fact that these compounds had a transient

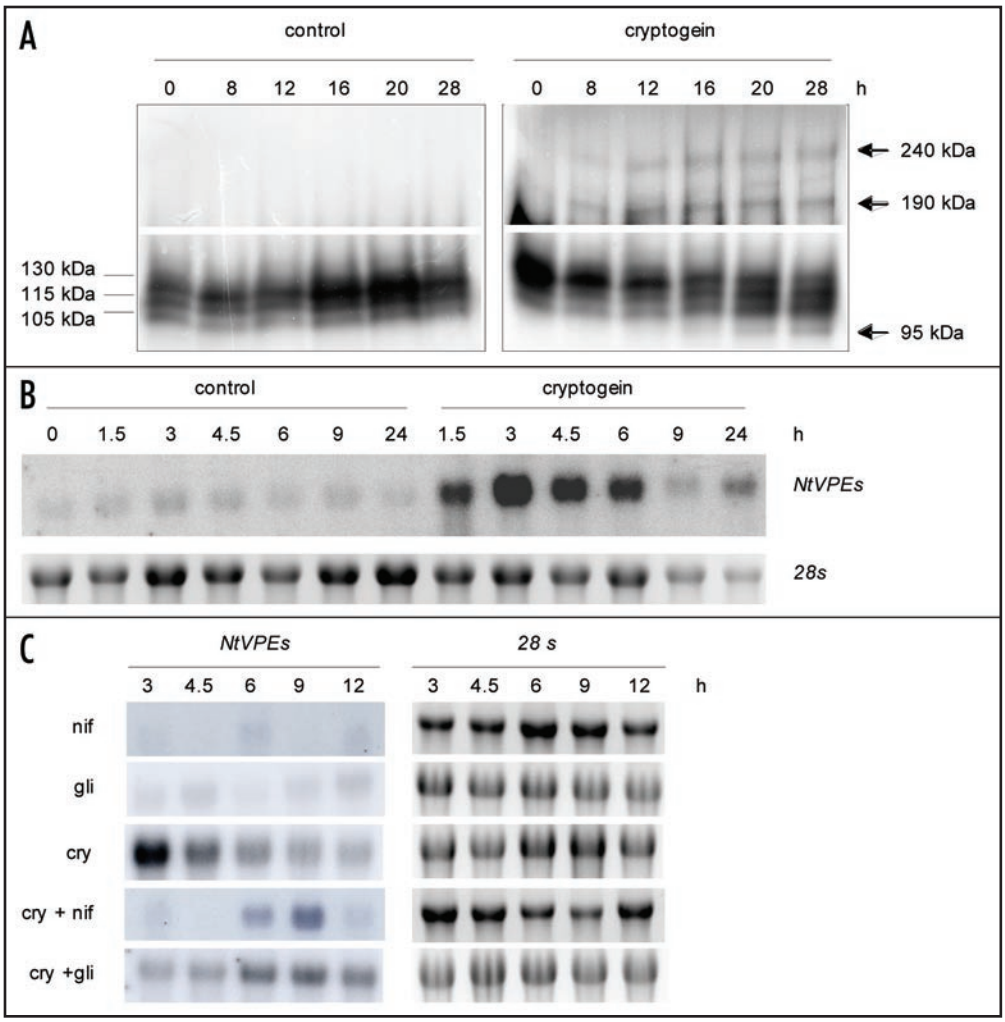

Figure 5. Contribution of cryptogein-induced NO_3^- efflux in the regulation of proteases. (A) Activation of proteases during cryptogein treatment. Tobacco cell suspensions were treated with cryptogein (25 nM). Proteins were resolved by SDS-PAGE and assayed in-gel for proteolytic activity with gelatin as substrate. To improve the resolution of the bands, once the gels have been scanned, the upper and lower part of the resulting images were analyzed separately using the software Adobe PhotoShop (Adobe Systems Inc., San Jose, CA). Results are from one of 6 representative experiments. (B) Cryptogein induces *VPEs* mRNA accumulation. Tobacco cell suspensions were treated with cryptogein (25 nM). Transcripts accumulation was monitored by northern blotting using a *NtVPE-1b* 712 bp cDNA fragment. Ethidium bromide-stained *28S* rRNA is shown as a control for gel loading. The data are representative of four experiments. (C) Effect of niflumic acid and glibenclamide on cryptogein-induced *VPEs* transcripts accumulation. Niflumic acid (200 μM) and glibenclamide (200 μM) were added to cell suspensions 10 min before cryptogein (25 nM). mRNA accumulation was monitored by northern blotting as described in (A). Ethidium bromide-stained *28S* rRNA is shown as a control for gel loading. The data are representative of four experiments. cry, cryptogein; gli, glibenclamide; nif, niflumic acid.

inhibitory effect on the cryptogein-induced NO_3^- efflux. It is also noteworthy that the vacuole shrinkage did not occur uniformly in the population of cells exposed to cryptogein. That is, the percentage of cells showing a significant loss of vacuole volume increased with time and reached a maximum of 65% after 10 h of elicitor treatment. The use of non synchronized cell cultures might explain the lack of uniformity in the response. Indeed, although cryptogein recognition occurs at all phases of the cell cycle, the elicitor-triggered responses quantitatively change according to the cell cycle phase.[46] Finally, it is worth pointing out that while most of the cells showing vacuole volume loss died, a few of them recovered their initial volume and, at least during our analysis, escaped cell death (data not shown). This observation suggests that these cells were able to develop efficient volume-rescuing regulatory mechanisms. Whether these cells were in a particular phase of the cell cycle remains to be established. Such remark also highlights that in cells unable to compensate the cryptogein-induced vacuole shrinkage, the volume compensatory mechanisms might be overridden or repressed.

We previously demonstrated that cryptogein induces a fast and long lasting Ca^{2+} influx sensitive to the Ca^{2+} surrogate La^{3+}, a common inhibitor of plasma membrane Ca^{2+} channels. Addition of La^{3+} in the mid-course of cryptogein treatment suppressed almost immediately cryptogein-induced early and late cellular events, indicating that Ca^{2+} influx from the extracellular space is required for the initiation and maintenance of the defence responses.[6,16,18,41] We also reported that this Ca^{2+} influx is a prerequisite for the activation of the NO_3^- efflux in cryptogein-treated cells.[23] Here, we present experiments showing that the NO_3^- efflux contributes to the elicitor-induced Ca^{2+} influx and increase in $[Ca^{2+}]_{cyt}$. Taken together, these data highlight the complexity of the functional links between Ca^{2+} and NO_3^- fluxes in transduction processes. A simple explanation might be that a first and fast Ca^{2+} influx is required for the activation of the NO_3^- efflux. In turn, the Ca^{2+}-activated NO_3^- efflux and the ensuing plasma membrane depolarization amplify the cryptogein signal by activating plasma membrane Ca^{2+} channels, resulting in a higher Ca^{2+} influx (Fig. 6). Two main arguments support this assumption. First, Kadota et al.[36] identified two putative voltage-dependent Ca^{2+} channels (NtTPC1A and NtTPC1B) involved in cryptogein-induced Ca^{2+} fluxes. Impairing the expression of both proteins caused a dramatic reduction of the elicitor-mediated increase in $[Ca^{2+}]_{cyt}$. Second, we previously showed that the NO_3^- efflux acts upstream of the elicitor-induced plasma membrane NADPH oxidase responsible for ROS production.[23] In turn, the H_2O_2 derived from NADPH oxidase activity participates in the increase of $[Ca^{2+}]_{cyt}$, probably through the activation of plasma membrane Ca^{2+} channels.[6] Collectively, these data suggest that the efflux of NO_3^- triggered by cryptogein leads to the activation of at least two types of Ca^{2+} channels, voltage- and ROS-dependent Ca^{2+} channels. The prime role of Ca^{2+}-dependent plasma membrane anion channels in amplifying Ca^{2+} signalling has been described in various mammalian cell types. For instance, in smooth muscle cells, Ca^{2+}-activated Cl^- channels (Cl_{Ca}), which are activated by a rise of $[Ca^{2+}]_{cyt}$, initiate a positive feedback

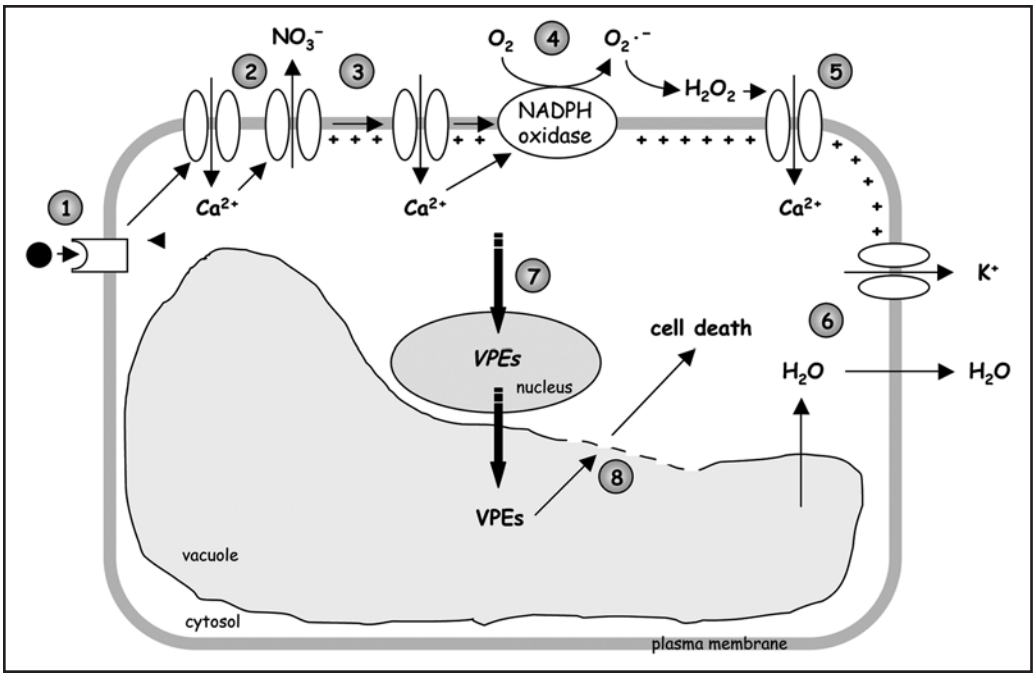

Figure 6. Hypothetical scheme for permeable anion channels functions in cryptogein signaling in tobacco cells. Cryptogein binding to high affinity binding sites (1) is followed by a first and fast Ca^{2+} influx leading to the activation of NO_3^--permeable anion channels (2). The anion efflux contributes to the depolarization of the plasma membrane (3) which, consequently, activates voltage-dependent plasma membrane Ca^{2+} channels. The resulting increase of $[Ca^{2+}]_{cyt}$ and/or amplification of plasma membrane depolarization promote the activation of NADPH oxidase (4) responsible for the production of ROS which, in turn, activate H_2O_2-sensitive Ca^{2+}-permeable channels from the plasma membrane (5). The large efflux of anions would also lead to K^+ and water effluxes from tobacco cells, inducing a loss of vacuolar volume (6). NO_3^- efflux, most probably through the resulting increase of $[Ca^{2+}]_{cyt}$ is also required for activation of genes encoding the vacuolar proteases *VPEs* (7). Once activated, VPEs might promote vacuolar-organized PCD, that is the activation of hydrolytic enzymes including proteases, nucleases and lipases involved in the collapse of vacuolar membranes and, ultimately, in cell death through the degradation of cytosolic and nuclear components (8).

loop mechanism whereby the membrane depolarization induced by these channels causes a Ca^{2+} influx through voltage-dependent Ca^{2+}-channels which sustain the depolarization by maintaining activation of Cl_{Ca}.[47] Interestingly, this signalling cascade is suppressed by niflumic acid, the most potent Cl_{Ca} channel blocker. Based on this model, our previous observation that adding Ca^{2+}-channel blockers during cryptogein treatment rapidly stopped the NO_3^- efflux[23] argues for the occurrence of a similar positive feedback loop.

The inhibitory effect of cycloheximide on cryptogein-induced cell death indicates that the HR is an active process requiring protein synthesis, a hallmark of PCD. To further assess the mechanisms by which the NO_3^- efflux contributes to cell death, we explored whether the anion efflux participated in the activation of proteases. The study was based on the finding that in various mammalian cell types, AVD, which is mediated by water loss caused by activation of the Cl^- channels and the ensuing K^+ efflux, precedes biochemical apoptotic events including protease activation.[25,48] We therefore characterized three active proteases, P95, P190 and P240, specifically detected in proteins extracted from cryptogein-treated cells. Their inactivation by the protease inhibitor PMSF was accompanied by a strong reduction of cell death, suggesting that the P95, P190 and P240 might take part in the mechanisms leading to the HR. This suggestion was also supported by the observation that cycloheximide strongly affected both their expression and the elicitor-induced cell death. However, none of these proteases appeared to be regulated through an NO_3^- efflux-dependent process. Their identity is currently unknown. The finding that their proteolytic activities were insensitive to the general caspase inhibitor Z-FAD-fmk and completely suppressed by the serine protease inhibitor PMSF, suggests that the P95, P190 and P240 are related to serine proteases and not caspase-like proteases. However, because of the questionable specificity of PMSF and, more generally, of protease inhibitors,[49] this assumption should be taken with caution.

The observation that Z-FAD-fmk partly reduced cryptogein-triggered cell death led us to extend our analysis to VPEs, a family of vacuolar cystein proteases exhibiting caspase-1 like activity and mediating the HR.[8] It has been proposed that VPEs promote the so-called vacuolar-organized PCD; that is the activation of hydrolytic enzymes including proteases, nucleases and lipases involved in the collapse of vacuolar membranes and the subsequent degradation of cytosolic and nuclear components.[50] Our results show that cryptogein treatment transiently and strongly up-regulated the expression of *VPEs*. In the presence of niflumic acid or glibenclamide, the accumulation of *VPEs* transcripts was clearly reduced and delayed. These data lead us to favor the hypothesis that the activation of cryptogein-induced NO_3^- efflux is an early prerequisite for VPEs synthesis (Fig. 6). Once activated, VPEs might mediate the NO_3^- efflux-dependent cell death by contributing to vacuolar-organized PCD. Additional experiments including the study of the elicitor's effects on anion channels or VPE-defective tobacco mutants will be necessary to support such an assumption.

In summary, this work extend our previous study showing that NO_3^- efflux is a key step in the signalling cascade leading to cryptogein induced-cell death and provide evidence that the movements of anions is tightly correlated with cellular and molecular events playing an important role in this process (Fig. 6). Furthermore, this finding highlights the notion that both plants and animals use anion channels as a component of cell death pathways.

References

1. Scheel D. Resistance response physiology and signal transduction. Curr Opin Plant Biol 1998; 1:305-10.
2. Grant M, Lamb C. Systemic immunity. Curr Opin Plant Biol 2006; 9:414-20.
3. Lam E, Kato N, Lawton M. Programmed cell death, mitochondria and the plant hypersensitive response. Nature 2001; 411:848-53.
4. Lam E. Controlled cell death, plant survival and development. Nat Rev Mol Cell Biol 2004; 5:305-15.
5. Greenberg JT, Yao N. The role and regulation of programmed cell death in plant-pathogen interactions. Cell Microbiol 2004; 6:201-11.
6. Lecourieux D, Mazars C, Pauly N, Ranjeva R, Pugin A. Analysis and effects of cytosolic free calcium increases in reponse to elicitors in *Nicotiana plumbaginifolia* cells. Plant Cell 2002; 14:2627-41.
7. Wendehenne D, Durner J, Klessig DF. Nitric oxide: A new player in plant signalling and defence responses. Curr Opin Plant Biol 2004; 7:449-55.
8. Hatsugai N, Kuroyanagi M, Yamada K, Meshi T, Tsuda S, Kondo M, Nishimura M, Hara-Nishimura I. A plant vacuolar protease, VPE, mediates virus-induced hypersensitive cell death. Science 2004; 305:855-58.
9. Lam E. Vacuolar proteases livening up programmed cell death. Trends Cell Biol 2005; 15:124-7.
10. Nürnberger T, Brunner F, Kemmerling B, Piater L. Innate immunity in plants and animals: Striking similarities and obvious differences. Immunol Rev 2004; 198:249-66.
11. Ponchet M, Panabieres F, Milat ML, Mikes V, Montillet JL, Suty L, Triantaphylides C, Tirilly Y, Blein JP. Are elicitins cryptograms in plant-Oomycete communications? Cell Mol Life Sci 1999; 56:1020-47.
12. Keller H, Blein JP, Bonnet P, Ricci P. Physiological and molecular characteristics of elicitin-induced systemic acquired resistance in tobacco. Plant Physiol 1996; 110:365-76.
13. Bourque S, Binet MN, Ponchet M, Pugin A, Lebrun-Garcia A. Characterization of the cryptogein binding sites on plant plasma membranes. J Biol Chem 1999; 274:34699-705.
14. Wendehenne D, Binet MN, Blein JP, Ricci P, Pugin A. Evidence for specific, high-affinity binding sites for a proteinaceous elicitor in tobacco plasma membrane. FEBS 1995; 374:203-7.
15. Garcia-Brugger A, Lamotte O, Vandelle E, Bourque S, Lecourieux D, Poinssot B, Wendehenne D, Pugin A. Early signaling events induced by elicitors of plant defenses. Mol Plant Microbe Interact 2006; 19:711-24.
16. Tavernier E, Wendehenne D, Blein JP, Pugin A. Involvement of free calcium in action of cryptogein, a proteinaceous elicitor of hypersensitive reaction in tobacco cells. Plant Physiol 1995; 109:1025-31.
17. Lamotte O, Courtois C, Dobrowolska G, Besson A, Pugin A, Wendehenne D. Mechanisms of nitric-oxide-induced increase of free cytosolic Ca^{2+} concentration in *Nicotiana plumbaginifolia* cells. Free Radic Biol Med 2006; 40:1369-76.
18. Lamotte O, Gould K, Lecourieux D, Sequeira-Legrand A, Lebun-Garcia A, Durner J, Pugin A, Wendehenne D. Analysis of nitric oxide signaling functions in tobacco cells challenged by the elicitor cryptogein. Plant Physiol 2004; 135:516-29.
19. Binet MN, Humbert C, Lecourieux D, Vantard M, Pugin A. Disruption of microtubular cytoskeleton induced by cryptogein, an elicitor of hypersensitive response in tobacco cells. Plant Physiol 2001; 125:564-72.
20. Hirasawa K, Amano T, Shioi Y. Effects of scavengers for active oxygen species on cell death by cryptogein. Phytochemistry 2005; 66:463-8.
21. Barbier-Brygoo H, Vinauger M, Colcombet J, Ephritikhine G, Frachisse JM, Maurel C. Anion channels in higher plants: Functional characterization, molecular structure and physiological role. Biochim Biophys Acta 2000; 1465:199-218.
22. Roberts KS. Plasma membrane anion channels in higher plants and their putative functions in roots. New Phytol 2006; 169:647-66.
23. Wendehenne D, Lamotte O, Frachisse JM, Barbier-Brygoo H, Pugin A. Nitrate efflux is an essential component of the cryptogein signaling pathway leading to defense responses and hypersensitive cell death in tobacco. Plant Cell 2002; 14:1937-51.
24. Yu SP, Choi DW. Ions, cell volume, and apoptosis. Proc Natl Acad Sci USA 2000; 97:9360-2.
25. Okada Y, Shimizu T, Maeno E, Tanabe S, Wang X, Takahashi N. Volume-sensitive chloride channels involved in apoptotic volume decrease and cell death. J Membr Biol 2006; 209:21-9.
26. Klüsener B, Weiler EW. Pore-forming properties of elicitors of plant defense reactions and cellulolytic enzymes. FEBS Lett 1999; 459:263-6.
27. Carden DE, Felle HH. The mode of action of cell wall-degrading enzymes and their interference with Nod factor signalling in *Medicago sativa* root hairs. Planta 2003; 216:993-1002.
28. Chandler MT, Tandeau de Marsac N, De Kouchkovsky Y. Photosynthetic growth of tobacco cells in liquid suspension. Can J Bot 1972; 50:2265-70.
29. Bonnet P, Bourdon E, Ponchet M, Blein JP, Ricci P. Acquired resistance triggered by elicitins in tobacco and other plants. Eur J Plant Pathol 1996; 102:181-92.
30. Reboutier D, Bianchi M, Brault M, Roux C, Dauphin A, Rona JP, Legue V, Lapeyrie F, Bouteau F. The indolic compound hypaphorine produced by ectomycorrhizal fungus interferes with auxin action and evokes early responses in nonhost Arabidopsis thaliana. Mol Plant Microbe Interact 2002; 15:932-8.
31. Solomon M, Belenghi B, Delledonne M, Menachem E, Levine A. The involvement of cysteine proteases and protease inhibitor genes in the regulation of programmed cell death in plants. Plant Cell 1999; 11:431-43.
32. Bradford MM. A rapid and sensitive method for the quantification of microgram quantities of protein utilizing the principle of protein-dye binding. Anal Biochem 1976; 72:248-54.
33. Church GM, Gilbert W. Genomic sequencing. Proc Natl Acad Sci USA 1984; 81:1991-5.
34. Schroeder JI, Keller BU. Two types of anion channel currents in guard cells with distinct voltage regulation. Proc Natl Acad Sci USA 1992; 89:5025-9.
35. Hedrich R, Busch H, Raschke K. Ca^{2+} and nucleotide dependent regulation of voltage dependent anion channels in the plasma membrane of guard cells. EMBO J 1990; 9:3889-892.
36. Kadota Y, Furuichi T, Ogasawara Y, Goh T, Higashi K, Muto S, Kuchitsu K. Identification of putative voltage-dependent Ca^{2+}-permeable channels involved in cryptogein-induced Ca^{2+} transients and defense responses in tobacco BY-2 cells. Biochem Biophys Res Commun 2004; 317:823-30.
37. Vandelle E, Poinssot B, Wendehenne D, Bentejac M, Pugin A. Integrated signaling network involving calcium, nitric oxide, and active oxygen species but not mitogen-activated protein kinases in BcPG1-elicited grapevine defenses. Mol Plant Microbe Interact 2006; 19:429-40.
38. Plasek J, Sigler K. Slow fluorescent indicators of membrane potential: A survey of different approaches to probe response analysis. J Photoch Photobiol B 1996; 33:101-24.
39. Rojo E, Martin R, Carter C, Zouhar J, Pan S, Plotnikova J, Jin H, Paneque M, Sanchez-Serrano JJ, Baker B, Ausubel FM, Raikhel NV. VPEgamma exhibits a caspase-like activity that contributes to defense against pathogens. Curr Biol 2004; 14:1897-906.
40. Hara-Nishimura I, Hatsugai N, Nakaune S, Kuroyanagi M, Nishimura M. Vacuolar processing enzyme : An executor of plant cell death. Curr Opin Plant Biol 2005; 8:404-8.
41. Pugin A, Frachisse JM, Tavernier E, Bligny R, Gout E, Douce R, Guern J. Early events induced by the elicitor cryptogein in tobacco cells: Involvement of a plasma membrane NADPH oxidase and activation of glycolysis and the pentose phosphate pathway. Plant Cell 1997; 9:2077-91.
42. Cho MH, Spalding EP. An anion channel in *Arabidopsis* hypocotyls activated by blue light. Proc Natl Acad Sci USA 1996; 93:8134-8.
43. Brault M, Amiar Z, Pennarun AM, Monestiez M, Zhang Z, Cornel D, Dellis O, Knight H, Bouteau F, Rona JP. Plasma membrane depolarization induced by abscisic acid in Arabidopsis suspension cells involves reduction of proton pumping in addition to anion channel activation, which are both Ca^{2+}dependent. Plant Physiol 2004; 135:231-43.
44. Roelfsema MR, Levchenko V, Hedrich R. ABA depolarizes guard cells in intact plants, through a transient activation of R- and S-type anion channels. Plant J 2004; 37:578-88.
45. Ward JM, Pei ZM, Schroeder JI. Roles of ion channels in initiation of signal transduction in higher plants. Plant Cell 1995; 7:833-44.
46. Kadota Y, Watanabe T, Fujii S, Maeda Y, Ohno R, Higashi K, Sano T, Muto S, Hasezawa S, Kuchitsu K. Cell cycle dependence of elicitor-induced signal transduction in tobacco BY-2 cells. Plant Cell Physiol 2005; 46:156-65.
47. Leblanc N, Ledoux J, Saleh S, Sanguinetti A, Angermann J, O'Driscoll K, Britton F, Perrino BA, Greenwood IA. Regulation of calcium-activated chloride channels in smooth muscle cells: A complex picture is emerging. Can J Physiol Pharmacol 2005; 83:541-56.
48. Maeno E, Ishizaki Y, Kanaseki T, Hazama A, Okada Y. Normotonic cell shrinkage because of disordered volume regulation is an early prerequisite to apoptosis. Proc Natl Acad Sci USA 2000; 97:9487-92.
49. van der Hoorn RAL, Jones JDG. The plant proteolytic machinery and its role in defence. Curr Opin Plan Biol 2004; 7:400-7.
50. Yamada K, Shimada T, Nishimura M, Hara-Nishimura I. A VPE family supporting various vacuolar functions in plants. Physiol Plant 2005; 123:369-75.